fishes

MDPI

Article

Decoding Vitellogenin Subtype Responses: A Molecular Approach to Biomarkers of Endocrine Disruption in *Scatophagus argus*

Meiqin Wu [1,2], Jun Zhang [1,2], Di Wu [1], Amina S. Moss [3,*] and Weilong Wang [1,4,5,*]

1 Building of China-ASEAN Belt and Road Joint Laboratory on Mariculture Technology, Shanghai 201306, China; mqwu@shou.edu.cn (M.W.); m240300990@st.shou.edu.cn (J.Z.); m220100242@st.edu.cn (D.W.)
2 College of Oceanography and Ecological Science, Shanghai Ocean University, Shanghai 201306, China
3 Institute of Aquaculture, University of Stirling, Stirling FK9 4LA, UK
4 Centre for Research on Environmental Ecology and Fish Nutrition of the Ministry of Agriculture, Shanghai 201306, China
5 Key Laboratory of Aquaculture Nutrition and Feed (Ministry of Agriculture and Rural Affair), Key Laboratory of Mariculture (Ministry of Education), Ocean University of China, Qingdao 266003, China
* Correspondence: amina.moss@stir.ac.uk (A.S.M.); wangweilong@shou.edu.cn (W.W.)

Abstract: Vitellogenins (Vtgs) are key yolk precursor proteins in fish, serving as critical indicators of gonadal maturation in females and reliable biomarkers for detecting xeno-oestrogenic pollution, particularly through their expression in juveniles or males. The *vtg* gene family comprises multiple subtypes that are species-specific, necessitating precise characterisation and quantification for effective use as biomarkers in studies on estrogenic endocrine-disrupting chemicals (EEDCs). In this study, we successfully cloned and characterised the full-length cDNAs of three *vtg* subtypes (*vtgAa*, *vtgAb*, and *vtgC*) from *Scatophagus argus*. Differential expression analysis revealed that *vtgAb* exhibited the highest responsiveness to 17α-ethynylestradiol (EE2) exposure, with a 3-fold increase in vivo at 10.0 μg/g EE2 and a 30-fold increase in vitro at 10^{-7} mol/L EE2. The expression patterns were dose- and time-dependent, with peak expression observed 72 h post-exposure. While in vivo assays indicated moderate upregulation, in vitro experiments demonstrated significantly higher expression, attributed to direct hepatocyte interaction with EE2. These findings confirm *vtgAb* as the most responsive subtype to oestrogen exposure in *S. argus* and highlight the species' tolerance to EE2, as compared to more sensitive species like *Danio rerio*. This study shows the evolutionary conservation of *vtg* transcripts across teleost species and reinforces the importance of subtype-specific characterisation to advance their application as biomarkers for EEDCs, with significant implications for environmental monitoring and pollution regulation.

Keywords: *Scatophagus argus*; vitellogenin; 17 α-ethynylestradiol; in vivo; in vitro

Key Contribution: The findings of this study have significant aquaculture environmental implications by demonstrating the use of *vtg* gene subtypes, particularly *vtgAb*, as sensitive biomarkers for detecting estrogenic endocrine-disrupting chemicals (EEDCs) in aquatic environments. The dose- and time-dependent expressions of *vtg* in response to EE2 exposure highlight their utility in monitoring pollution and assessing ecosystem health. The conserved nature of Vtg amino acids across teleost species enhances their applicability in broader ecological studies. This research provides a foundation for

Academic Editor: Zhihua Li

Received: 24 November 2024
Revised: 15 December 2024
Accepted: 24 December 2024
Published: 31 December 2024

Citation: Wu, M.; Zhang, J.; Wu, D.; Moss, A.S.; Wang, W. Decoding Vitellogenin Subtype Responses: A Molecular Approach to Biomarkers of Endocrine Disruption in *Scatophagus argus*. *Fishes* **2025**, *10*, 15. https://doi.org/10.3390/fishes10010015

improved environmental monitoring and protection strategies against EEDCs, aiding in safeguarding fish populations and maintaining the ecological balance of aquatic systems

1. Introduction

In recent decades, increasing attention has been directed towards evaluating the adverse ecological effects of endocrine-disrupting chemicals (EDCs), particularly within aquatic environments [1]. EDCs are exogenous substances or mixtures, either natural or synthetic, that are discharged from chemical pollutants or excreted in vertebrate waste [2]. These compounds can accumulate in surface and ground waters through hydrological processes [3]. Long-term accumulation, even at low concentrations, has the potential to exert adverse impacts on both human health and ecosystems. Moreover, EDCs pose significant challenges to the One Health framework, which emphasises the interconnectedness of human, animal, and environmental health. Among EDCs, estrogenic endocrine-disrupting chemicals (EEDCs) have garnered significant concern due to their effects on reproductive success in vertebrates, particularly fish [4]. EEDCs induce feminisation in male fish by altering courtship behaviour, delaying testicular maturation, and causing the development of feminised phenotypes, such as the production of oogonia and vitellogenin (Vtg) [5]. The resulting skewed sex ratios have been documented in numerous fish species, leading to biodiversity loss, compromised food security, economic consequences, and altered ecosystem dynamics, ultimately causing widespread ecological damage [6].

The ubiquitous presence of EEDCs, including natural oestrogenic steroids such as 17 β-oestradiol (E2), an endogenous hormone regulating reproductive processes in fish, particularly females, has been well documented. Detection frequencies of E2 in natural waters worldwide range from 53% to 83%, with concentrations between 48 and 370 μg/L [6,7]. Synthetic derivatives of natural oestrogens, such as 17α-ethynylestradiol (EE2), commonly used in oral contraceptives and hormone replacement therapies, have a proportionally greater environmental impact than E2, as indicated by monitoring studies published since 2015 [1–8]. The increasing use of both natural and synthetic oestrogens in human medicine and animal agriculture has exacerbated these impacts. However, it remains challenging to detect total EEDCs or predict their ecological metabolic dynamics using random water samples due to their diverse forms and complex interactions in aquatic systems [9]. Various aquatic species, particularly fish, are commonly employed in bioassays to indirectly assess the effects of these chemicals on ecosystems [10].

Vtg is a key precursor of yolk proteins, synthesised under the regulation of the hypothalamus–pituitary–gonad axis through the activation of oestrogen receptors [11]. Vtg is predominantly produced in the liver of female oviparous vertebrates during the reproductive phase in response to endogenous oestrogen [12]. There is a strong positive correlation between circulating E2 levels and the transcription, expression, and synthesis of Vtg in liver tissues during gonadal development [13]. Additionally, exposure to exogenous oestrogen or oestrogen-like compounds can markedly induce *vtg* gene expression and elevate Vtg production in both immature females and male fish. As a result, *vtg*/Vtg expression levels serve not only as an indicator of gonadal maturation in females but also as a reliable biomarker for assessing xeno-oestrogenic pollution, particularly through the detection of *vtg*/Vtg expression in male fish [14,15]. Structurally, Vtg consists of major functional domains: the lipovitellin heavy chain (LvH), phosvitin (PV), lipovitellin light chain (LvL), β′-component, and C-terminal peptide [5]. LvH and LvL function as reservoirs for proteins and lipids essential for embryonic growth, while PV, a highly phosphorylated domain, is critical for mineral storage, including calcium and

phosphate, required for skeletal and tissue development. However, the functions of the β′-component and C-terminal peptide in embryonic nutrition or physiology remain unknown. Collectively, these domains highlight Vtg's pivotal role in reproduction and embryogenesis [7].

Current methods for detecting and quantifying fish Vtg are often developed based on a single, unclassified form of Vtg [16]. However, various *vtg* transcript subtypes have been identified and classified according to their function in different species, including the grey mullet (*Mugil cephalus*) [17], Japanese common goby (*Acanthogobius flavimanus)* [18], medaka (*Oryzias latipes*) [19], mosquitofish (*Gambusia affinis*)[20], mummichog (*Fundulus heteroclitus*) [21], red seabream (*Pagrus major*) [15], tilapia (*Oreochromis mossambicus*) [22], and white perch (*Morone americana*) [14]. These findings demonstrate that *vtg*/Vtg subtypes are species-specific, and their characterisation and quantification are essential before utilising them as biomarkers in studies of EEDCs. However, the underlying mechanisms behind this atypical *vtg*/Vtg expression and synthesis remain unclear.

The spotted scat (*Scatophagus argus*) is a commercially valuable species commonly found in the East and South China Seas. Renowned for its tasty and nutritious flesh, it is highly sought after in local markets for consumption [23]. To date, no classification of Vtg subtypes has been reported for *S. argus*. In this study, the full-length cDNA sequences of three *S. argus vtg* subtypes (*vtgAa*, *vtgAb,* and *vtgC*) were successfully cloned using rapid amplification of cDNA ends (RACE) technology. Gene and protein structural data were analysed to infer the function roles of these genes and their potential impacts on reproduction in *S. argus*. Additionally, the differential expression of *vtgAa*, *vtgAb*, and *vtgC* mRNA was examined both in vivo and in vitro following an intraperitoneal injection of EE2 and exposure of hepatocytes to EE2. These analyses elucidated the molecular mechanisms underlying Vtg's role in reproductive regulation. These findings highlight the critical importance of species-specific Vtg subtype characterisation for accurately monitoring EEDCs in aquatic environments. By demonstrating the subtype-specific expression of Vtg in response to estrogenic substances, this study highlights the potential of Vtg subtypes as sensitive biomarkers for detecting oestrogen contamination and assessing ecosystem health. Ultimately, this research establishes a foundation for advancing environmental monitoring techniques and contributes to safeguarding aquatic biodiversity.

2. Materials and Methods

2.1. Experimental Animals and Conditions

One hundred and fifty healthy juvenile *S. argus* (mean weight: 9 ± 0.2 g; mean body length: 4.7 ± 0.3 cm) were collected from Zhuhai Aquaculture Base (113 30′ N, 22 05′ E, Guangdong, China) for this study. The juveniles were acclimated in a 250 L recirculating tank and fed with commercial feed twice daily for three weeks. The water quality parameters were monitored daily, with the temperature maintained at 27 ± 1 °C, salinity at 30 ± 1%, dissolved oxygen levels ≥ 6.0 mg/L, and a 12 L:12 D photoperiod.

2.2. Sampling Techniques

In the in vivo experiment, juvenile *S. argus* were divided into five 250 L tanks, comprising four EE2 treatment groups and one control group (n = 25 per group). Following a 2-day acclimation period, the fish received a single intraperitoneal injection of EE2 (Sigma-Aldrich, St. Louis, MO, USA), dissolved in absolute ethanol, at different doses (0.01, 0.1, 1, and 10 μg/g body weight). The control group was injected with absolute ethanol. Before sampling, the fish were deeply anaesthetised using MS-222 (Sigma-Aldrich, St. Louis, USA) at a concentration of 100 mg/L. Liver tissues were collected at 24,

48, 72, and 96 h post-injection. The samples were preserved in RNAlater (Ambion, Austin, TX, USA) overnight at 4 °C and then stored at −30 °C until further analysis.

2.3. Total RNA Extraction and cDNA Synthesis

Total RNA was extracted from liver tissues using Trizol Reagent (Invitrogen, USA). The integrity of the extracted RNA was assessed by agarose electrophoresis, and the RNA concentration was determined using a NanoDrop 2000c spectrophotometer (Thermo Scientific Inc., MA, USA). First-strand cDNA synthesis was carried out using Superscript II reverse transcriptase (Invitrogen, USA) and oligo d (T)16 (Promega, USA) mRNA primer with 1 μg of total RNA serving as the template. The reverse transcription reactions were conducted under the following conditions: 25 °C for 10 min, 42 °C for 60 min, and 85 °C for 5 min. The resulting cDNA was subsequently used as the template for gene cloning and quantitative real-time polymerase chain reaction (qRT-PCR) and was stored at −80 °C until further use.

2.4. Cloning of vtg Sequence from S. argus

Liver tissues sampled from five mature female *S. argus* individuals (body weight: 312.4 ± 38.7 g; gonadosomatic index: 10.3 ± 2.4%) were pooled prior to total RNA extraction to facilitate molecular cloning. Sequences of various teleost *vtg* genes were retrieved from the NCBI database, and conserved domains were identified through homology comparison. These domains were used to design degenerate primers for amplifying intermediate *vtg* fragments. PCR was conducted in a 25 μL reaction mixture containing 2.5 μL of 10 × buffer, 2.5 μL of MgCl2, 1.0 μL of dNTPs mix (2.5 mmol/L), 0.5 μL of each primer (10 μmol/L), 0.3 μL of Taq DNA Polymerase (5 U/μL), 1.0 μL of template, and nuclease-free water (ddH_2O) to reach a final volume of 25.0 μL. The amplification protocol included an initial denaturation at 94 °C for 3 min, followed by 30 cycles of denaturation at 94 °C for 45 s, annealing at 58 °C for 30 s, and extension at 72 °C for 90 s, with a final extension at 72 °C for 10 min.

The amplified products were analysed by a 1.5% agarose gel electrophoresis and purified using the GENECLEAN Turbo Kit (MP Biomedicals Europe, IIIkrich, France). The purified PCR products were ligated into the pGEM-T Easy vector (Promega, Madison, WI, USA) and transformed into *Escherichia coli* DH5α strain (Tiangen, Beijing, China). Positive clones were selected by blue-white plaque screening, and four positive clones from each sample were randomly chosen for sequence analysis, which was performed by Sangon Biotech Co., Ltd. (Shanghai, China).

The cDNA templates for 5′- and 3′-rapid amplification of cDNA ends (RACE) were synthesised from hepatic total RNA extracted from female *S. argus* using the SMARTer™ RACE cDNA Amplification Kit (Clontech, Takara Bio Inc., Shiga, Japan). RACE reactions were conducted using the universal primer mix (UPM) supplied by the kit, along with gene-specific primers (GSPs) designed based on the partial *vtg* cDNA sequences of *S. argus* (Table 1). The PCR amplification was carried out in a 25 μL reaction volume containing 2.5 μL of 10 × Advantage 2 PCR buffer, 0.5 μL of dNTPs mix (10 mM), 0.5 μL of GSP (10 μM), 2.5 μL of 10 × UPM, 1.25 μL of template, and 0.5 μL of 50 × Advantage 2 polymerase mix (Clontech, Japan). The amplification protocol consisted of 25 cycles of denaturation at 94 °C for 30 s, annealing at 68 °C for 30 s, and extension at 72 °C for 4 min, followed by a final extension at 72 °C for 10 min.

Following the cloning of the 5′ and 3′ ends of the *vtg* sequences via RACE, new gene-specific primers (Table 1) were designed to obtain full-length *vtg* sequences. Amplification was performed using the Advantage 2 PCR kit (Clontech, Japan) with the following components: 5 μL of 10 × Advantage 2 PCR buffer, 1 μL of dNTPs mix (10 mM), 1 μL each of forward and reverse gene-specific primers (10 μM), 1 μL of template, 1 μL of 50 ×

Advantage 2 polymerase mix, and ddH_2O to a finial volume of 50 μL. The PCR conditions included an initial denaturation at 95 °C for 1 min, followed by 35 cycles of 95 °C for 30 s and 68 °C for 3 min. This was followed by 25 cycles of 94 °C for 30 s, 68 °C for 30 s, and 72 °C for 3 min, with a final elongation step at 68 °C for 3 min. The resulting PCR products were subcloned into the pGEM-T Easy vector and sequenced for further analysis.

RACE primers were designed based on the obtained intermediate fragment sequence (Table 1). Two-terminal amplification was performed following the protocols provided in the SMARTer™ RACE cDNA Amplification Kit (Clontech, Takara Bio Inc., Shiga, Japan). Initially, 5′-RACE-Ready cDNA and 3′-RACE-Ready cDNA were synthesised using the kit system and stored at −20 °C. Both types of cDNAs served as templates for amplification, with gene-specific primers (GSPs, Table 1) and the universal primer mix (UPM) provided by the kit used as primers.

The first-round of PCR products served as templates for the subsequent amplification, utilising the upstream nested primers NGSP1 and NUPM (supplied in the kit) serving as primers. The amplification was conducted under the following conditions: 25 cycles of denaturation at 94 °C for 30 s, annealing at 68 °C for 30 s, and extension at 72 °C for 4 min, followed by a final extension at 72 °C for 10 min. The resulting PCR products were subcloned into the pGEM-T Easy vector and subsequently sequenced by Sangon Biotech Co., Ltd.

Table 1. Primer sequences for PCR.

Primers	Sequences (5′-3′)	Purpose
vtgAa-F	ACTGYYKCWGGTCTKCCNATGGAGCT	Partial *vtgAa* cloning
vtgAa-R	AGCTTCTCYGCASCCTTWGGKCC	Partial *vtgAa* cloning
vtgAb-F	TTCTKGAGKTYGGAGYSMGADCTG	Partial *vtgAb* cloning
vtgAb-R	GCAGCWGYRAGRYCYTCMACATYT	Partial *vtgAb* cloning
vtgC-F	TWMRGCCVYTGSTGRAHATGG	Partial *vtgC* cloning
vtgC-R	AKYCCHTCHGSRCGRAYACC	Partial *vtgC* cloning
vtgAa-GSP1	CCTGGACCTTGGCTCTTGAGACTATGG	5′RACE for *vtgAa*
vtgAa-NGSP1	CCTTGGCTCTTGAGACTATGGCAGC	5′RACE for *vtgAa* (Nest)
vtgAa-GSP2	CGACCTCATCTGGAAAACACCAACAC	3′RACE for *vtgAa*
vtgAa-NGSP2	GCTGGCTTTACATCTTCCCATTGCTCTC	3′RACE for *vtgAa* (Nest)
vtgAb-GSP1	GCAGGAACGATTGTGTAAACTCTGGCTC	5′RACE for *vtgAb*
vtgAb-NGSP1	TGGAAGTTCTCAGGCAGAGGTGG	5′RACE for *vtgAb* (Nest)
vtgAb-GSP2	ACGCCTACTTGAGAAGCCTTGCC	3′RACE for *vtgAb*
vtgAb-NGSP2	CTGCTGGAGTTGGGTATCCGTGC	3′RACE for *vtgAb* (Nest)
vtgC-GSP1	AAGGCGGGCTTGTTGGCGGGCAG	5′RACE for *vtgC*
vtgC-NGSP1	CCTTCAGCACGGATACCCAACTCC	5′RACE for *vtgC* (Nest)
vtgC-GSP2	TGGGGAACGCAGGTCATCCAGGC	3′RACE for *vtgC*
vtgC-NGSP2	TTGCCACCTCGTGTGCTGAGTGC	3′RACE for *vtgC* (Nest)
vtgAa-full-F	GTATCAACGCAGAGTACATGGGGT	Full-length *vtgAa* cloning
vtgAa-full-R	AGATAGGTGACTGACAGGACAAAGTGTTA	Full-length *vtgAa* cloning
vtgAb-full-F	ATGGGGACATTCACCAGCCATGAGGGT	Full-length *vtgAb* cloning
vtgAb-full-R	GGGCAAGCAGTGGTATCAACGCAGAG	Full-length *vtgAb* cloning
vtgC-full-F	GTTTCACAAAGGATTTCTGGGT	Full-length *vtgC* cloning
vtgC-full-R	GTGGGAGAGGGACTGGAATAGC	Full-length *vtgC* cloning
vtgAa qPCR-F	TTTGCCACAATCTGCAGAGG	qRT-PCR for *vtgAa*
vtgAa qPCR-R	TCAAACTGAGCTGCTTTGCG	qRT-PCR for *vtgAa*
vtgAb qPCR-F	ATTCCCATTGACCTGCCAAG	qRT-PCR for *vtgAb*
vtgAb qPCR-R	AAAGCGGCATTGCGAGATTC	qRT-PCR for *vtgAb*
vtgC qPCR-F	TGCAGGGTCAAAATCGTTGG	qRT-PCR for *vtgC*
vtgC qPCR-R	TTTTCCCCGGAAAGCCATTG	qRT-PCR for *vtgC*

ef1-α qPCR-F	TGTGAAGCAGCTCATCGTTG	qRT-PCR for *ef1-α*
ef1-α qPCR-R	ATGTAGGTGCTCACTTCCTTGG	qRT-PCR for *ef1-α*

B = C/G/T, H = A/T/C, K = G/T, M = A/C, R = A/G, S = C/G, V = A/C/G, W = A/T, Y = C/T.

2.5. Sequence Analysis of vtgs

Following the cloning of the 5′ and 3′ ends of the *vtg* sequences via RACE, new gene-specific primers were designed to obtain consecutive full-length *vtg* sequences. Homology analysis of the deduced amino acid (AA) sequences of putative *S. argus* Vtgs was conducted using BLAST (https://blast.ncbi.nlm.nih.gov/Blast.cgi, accessed on 1 June 2023). The open reading frame (ORF) was identified using the ORF Finder tool (http://www.ncbi.nlm.nih.gov/orffinder). Prediction of a signal peptide was conducted using the SignalP4.1 Server (http://www.cbs.dtu.dk/services/SignalP/) [24]. The basic physical and chemical parameters of the protein were analysed using ProtParam (http://web.expasy.org/protparam). The phylogenetic analysis of vertebrate Vtgs AA sequences was carried out with the Neighbour Joining method implemented in MEGA version 10.0 software, with sequence alignment conducted in Clustal X version 2.0.1. Bootstrap values, based on 1000 replicates, are shown alongside the branches, representing the percentage of replicate trees in which the associated taxa clustered together. Evolutionary distances were calculated using the p-distance method, expressed as the number of amino acid differences per site. Positions containing gaps or missing data were excluded from the analysis.

2.6. Quantitative Real-Time Reverse Transcription PCR (qRT-PCR) of vtg mRNA Expression

The primers used for the qRT-PCR are listed in Table 1. Elongation factor 1-alpha (EF1-α) served as the internal reference gene. The qRT-PCR was conducted in a 20 μL reaction volume comprising 10.0 μL of SYBR Premix Ex Taq II (2×), 0.4 μL of upstream and downstream primers (10.0 umol/L), 1.0 μL of DNA template, and ddH_2O to reach a final volume of 20 μL. The amplification was performed in two stages: an initial pre-denaturation step at 95 °C for 30 s, followed by 40 cycles consisting of denaturation at 95 °C for 5 s and renaturation and extension at 60 °C for 34 s. A subsequent step included denaturation at 95 °C for 15 s, annealing at 60 °C for 1 min, and extension at 60 °C for 34 s. In addition, duplicate standard curves were generated using a serial dilution (in triplicate) of plasmid DNA containing the target gene (10^1–10^6 copies per reaction). The expression levels (copy number per reaction) of the target gene (*vtgs*) were normalised to the expression levels of the reference gene (*ef1-α*). The results were then reported as a fold change in abundance relative to the inter-assay control (IAC) values obtained in each reaction.

2.7. Hepatocyte Culture of S. argus

Hepatocytes were isolated using enzymatic digestion following the methodology outlined by Figueiredo et al. [25]. Venous blood was collected from the tail of *S. argus* following anaesthesia with 50 mg/L MS-222, after which the liver was aseptically dissected and removed. The liver tissue was washed three times with phosphate-buffered saline (PBS) containing dual antibiotics (100 IU/mL each of penicillin and streptomycin). The tissue was then minced into 1 mm^3 pieces and placed in a 15 mL centrifuge tube, where it was digested at 28 °C with 10.0 mL 0.25% trypsin. Following digestion, the cell suspension was filtered through a 100-mesh filter and centrifuged at 1000 rpm for 5 min. The resulting pellet was resuspended in Medium 199 (Sigma-Aldrich, St. Louis, USA) at an initial cell density of 5×10^5 cells/mL. The yield and immediate survival rate of hepatocytes were assessed using trypan blue staining under light microscopy. The hepatocytes were

cultured in flasks, with the culture medium replaced every 3–4 d, and maintained at 28 °C in a 2% (*v*/*v*) CO_2 atmosphere.

2.8. In Vitro Experiments

Hepatocytes from *S. argus* were cultured with M199 medium (GIBCO Laboratories, Grand Island, NY) supplemented with 15% (*v*/*v*) foetal bovine serum (FBS, HyClone Laboratories, Logan, USA) at 28 °C [26]. Once the cells reached approximately 70% confluence, they were detached using trypsin containing 0.25% EDTA and subsequently sub-cultured. Upon reaching the third passage, the hepatocytes were again digested with trypsin containing 0.25% EDTA and resuspended. After thorough mixing, 200 μL of the supernatant was transferred to 1.5 mL centrifuge tubes for trypan blue staining, while an additional 20 μL was used for cell counting with a haemocytometer. Cells were evenly seeded into a 24-well plate at a density of approximately 5×10^5 cells per well, with 1 mL of culture medium added to each well. The culture conditions were maintained at 28 °C. Once a monolayer was formed, the hepatocytes were exposed to EE2 at serial dilutions ranging from 10^{-11} to 10^{-5} mol/L [27]. The control group was only exposed to the solvent carrier (absolute ethanol). The gene expression of *vtg* was assessed at 24, 48, 72, and 96 h of incubation using qRT-PCR using the method described above.

2.9. Statistical Analysis

The results in the current study were reported as means ± standard deviation (n = 3). The data were subjected to a one-way ANOVA using SPSS 20.0 software. Duncan's multiple range test was used as a post hoc test. Differences among the treatments' means were considered significant at $p < 0.05$.

3. Results

3.1. Sequence Features of Vtg Analysis in S. argus

The *vtg* gene sequences of *S. argus* are presented in Figure S1. Full-length cDNA sequences of three *vtg* genes from the liver of *S. argus* were successfully cloned using RACE-PCR. Detailed information regarding the cDNAs of *S. argus* VtgAa, VtgAb, and VtgC, including their 5′ untranslated regions (UTRs), 3′-UTRs, open reading frames (ORFs), molecular weights (Mw), and isoelectric points (PI), is provided in Table 2. When compared with the protein structure of VtgA2 (NP_001038378) in *Danio rerio*, both VtgAa and VtgAb in *S. argus* exhibited the complete structure of Vtg (LvH, PV, and LvL), whereas VtgC lacked the PV structure (Figure 1).

Table 2. Information about *vtg* cDNA and AA sequences.

Gene	Full Length (bp)	ORF (bp)	Amino Acids (AA)	GenBank No	Molecular Weight (Mw) (kDa)	Isoelectric Point (PI)	Predicted N-Terminal Signal Peptide (N, AA)
vtgAa	5360	5091	1696	KY676847	186.07	9.16	15
vtgAb	5346	5100	1699	KY654346	186.37	9.24	15
vtgC	4244	3828	1275	KY676848	142.87	6.43	15

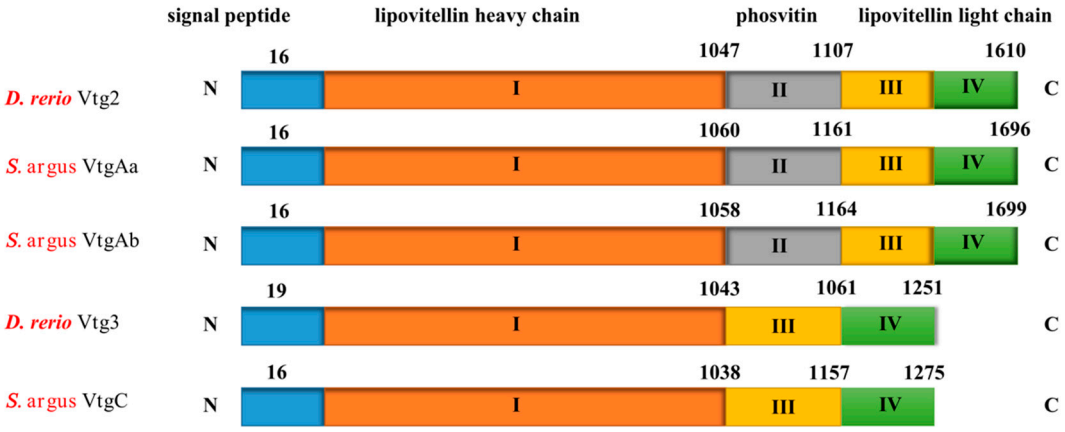

Figure 1. Diagrams of Vtg AA domains. *S. argus*-Vtg: VtgAa, VtgAb, VtgC and *D. rerio*-Vtg: Vtg2, Vtg3.

3.2. VtgAa, VtgAb, and VtgC AA Identity Analysis

When the *S. argus* VtgAa, VtgAb, and VtgC sequences were aligned with Vtgs from other teleost species, they showed the highest sequence identity with white perch (*M. americana)* at 83%, 85%, and 85%, respectively, based on identical sequences retrieved from the NCBI GenBank database. Comparatively, sequence identities with the red seabream (*P. major*) were slightly lower, at 81%, 82%, and 83%, respectively.

3.3. Systematic Evolution of S. argus VtgAa, VtgAb, and VtgC

The evolutionary relationships of *S. argus* VtgAa, VtgAb, and VtgC are illustrated in Figure 2. Phylogenetic trees were constructed using Vtg sequences from six different teleost species. VtgAa and VtgAb were grouped on a single branch, while VtgC was located on a separate branch. With the exception of *D. rerio*, VtgAa and VtgAb sequences from the other five teleost species clustered together on a single branch. *S. argus* exhibited the highest VtgAa sequence homology with *M. americana* and *P. major*, followed by *O. latipes*. For VtgAb, *M. americana* displayed the greatest sequence homology with *S. argus*, followed by *P. major* and *O. latipes*. In the case of VtgC, *P. major* displayed the highest homology with *S. argus*, followed by *M. americana* and *O. latipes*.

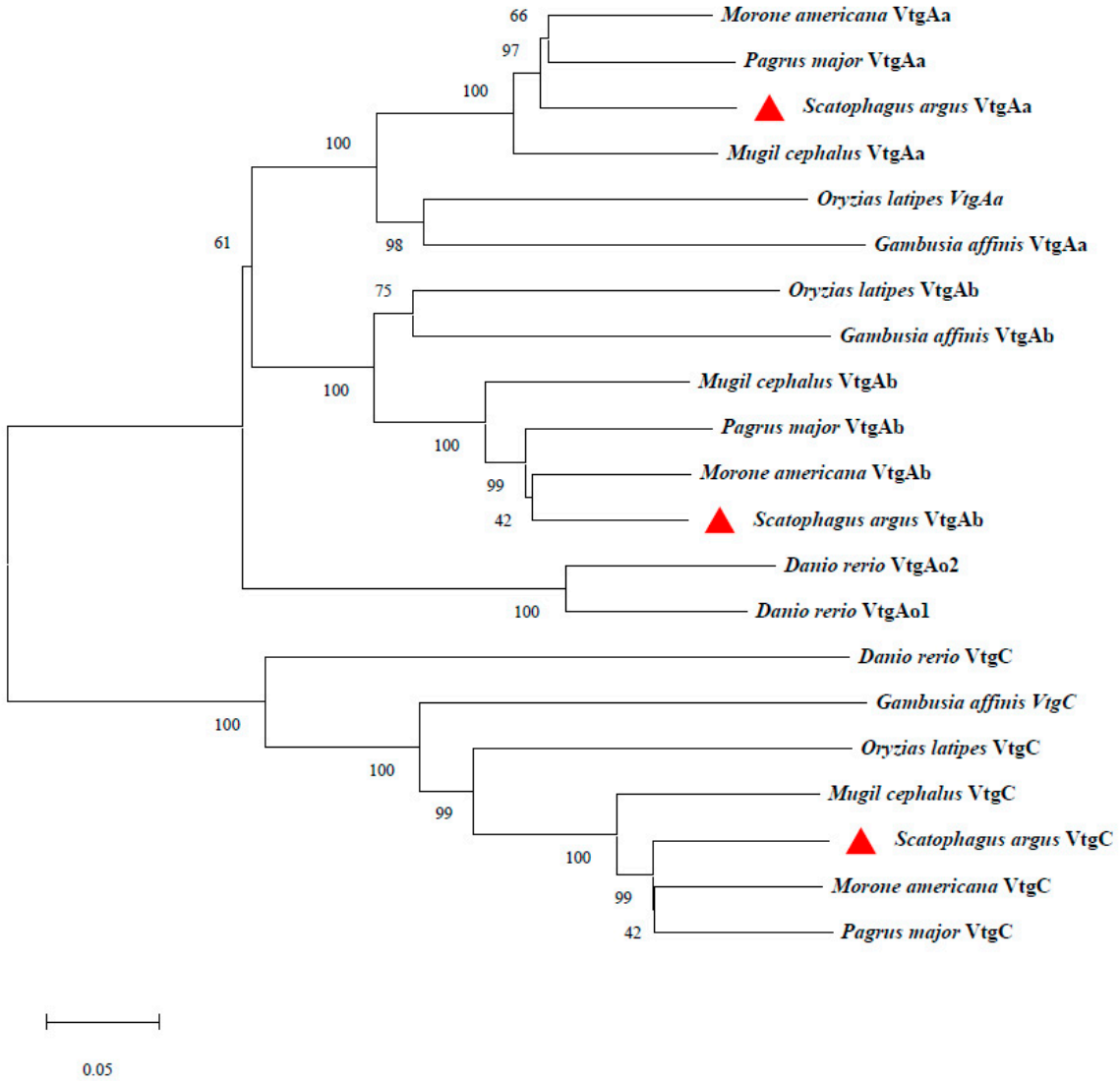

Figure 2. Phylogenetic inferences of the deduced AA sequence of Vtg in *S. argus* and various teleosts. GenBank accession number: *M. americana*-Vtg: Vtg Aa (AAZ17415.1), Vtg Ab (AAZ17416.1), Vtg C (AAZ17417.1); *O. latipes*-Vtg: Vtg Aa (BAB79696), Vtg Ab (BAB79591), Vtg C (ENSORLP00000008173); *P. major*-Vtg: Vtg Aa (BAE43870), Vtg Ab (BAE43871), Vtg C (BAE43872); *D. rerio*-Vtg: Vtg Ao1 (NP_001038362), Vtg Ao2 (NP_001038378), Vtg C (AAG30407); *G. affinis*-Vtg: Vtg Aa (BAD93697.1), Vtg Ab (BAD93698.1), Vtg C (BAD93699.1); *S. argus*-Vtg: Vtg Aa (KY676847), Vtg Ab (KY654346), Vtg C (KY676848). *M. cephalus*-Vtg: Vtg Aa (AB288932.1), Vtg Ab (AB288933.1), Vtg C (AB288934.1).

3.4. vtgs mRNA Expression In Vivo Following EE2 Therapy

qRT-PCR analysis revealed that the mRNA expression of *vtgAb* in liver tissue was consistently higher than that of the other two subtypes across numerous time points (24, 48, 72, and 96 h) and across a range of EE2 doses (0.01, 0.1, 1, and 10 μg/g) (Figure 3). Following the intraperitoneal injection of EE2, the *vtgAb* mRNA expression in liver tissues was higher at the 1 and 10 μg/g doses compared to the 0.01 and 0.1 μg/g doses. The *VtgAb* mRNA expression started at a low level at 24 h, peaked at 72 h, and gradually declined until the conclusion of the experiment at 96 h. The maximum mRNA expression of *vtgAb* in EE2-treated hepatocytes was observed at 72 h for the 10.0 μg/g concentration, with relative expression levels approximately increasing three times (Figure 4).

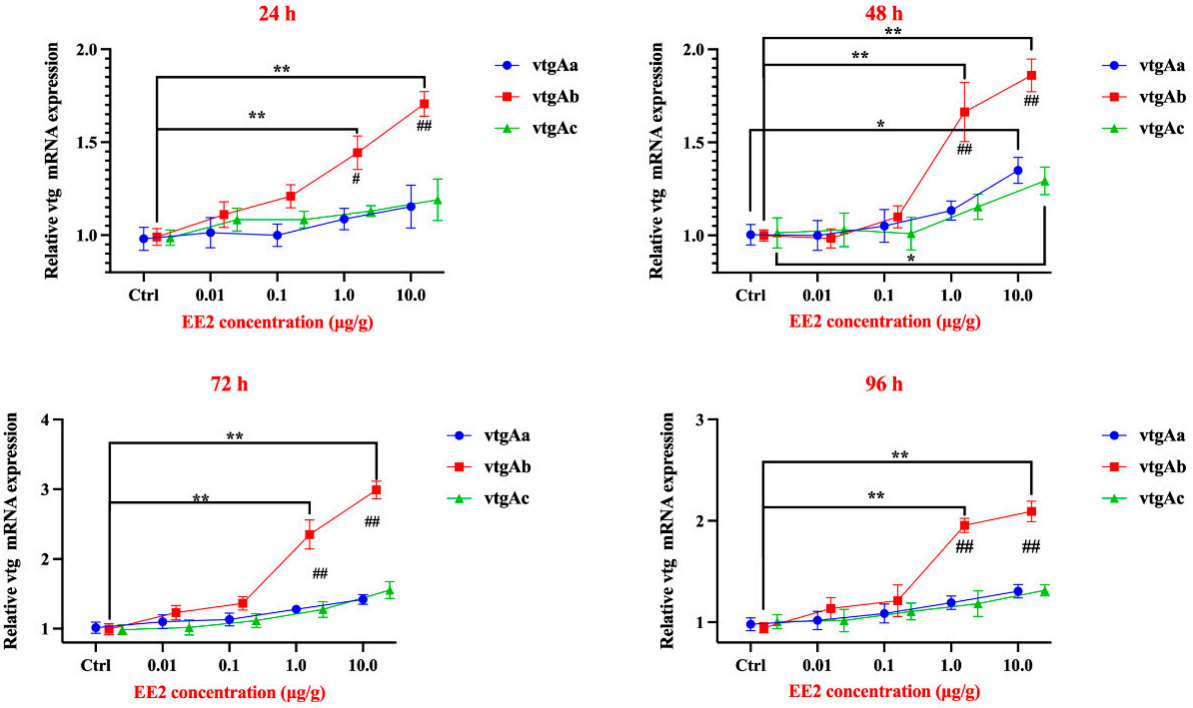

Figure 3. Analysis of *S. argus vtg* mRNA expression for different processing times and concentrations after injection to EE2. The asterisk above the data point represents significant difference, * $p < 0.05$, ** $p < 0.01$ vs. control (Ctrl). The well number below the data point represents significant difference, $^{\#}p < 0.05$, $^{\#\#}p < 0.01$ vs. 0.01 and 0.1 μg/g EE2 concentration groups.

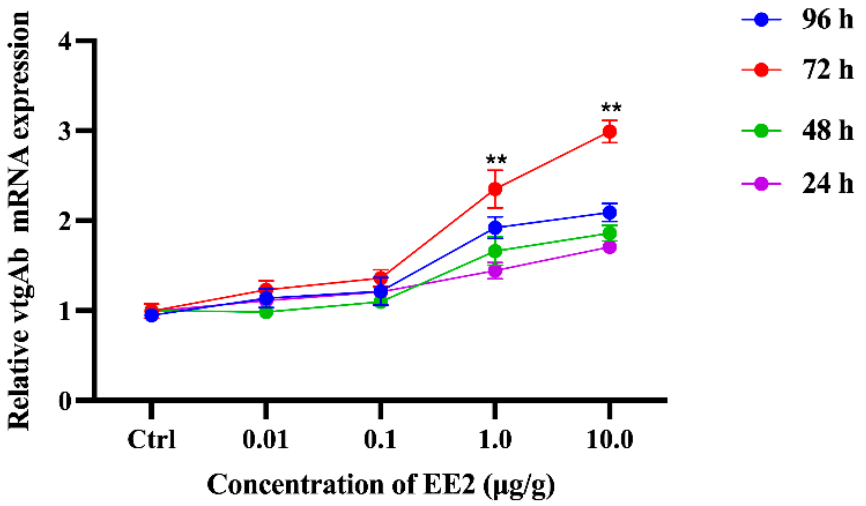

Figure 4. Analysis of *vtgAb* mRNA expression in *S. argus* for different processing times and concentrations after EE2 injection. The asterisk above the data point represents significant difference, * $p < 0.05$, ** $p < 0.01$ vs. control (Ctrl).

3.5. The mRNA Expression Analysis of vtgAb In Vitro After EE2 Treatment

To further validate the differential regulatory effects of oestrogen on *vtgAb* mRNA expression in vitro, primary hepatocytes from *S. argus* were treated with varying concentrations of EE2 for 24, 48, 72, and 96 h. Across concentrations ranging from 10^{-10} mol/L to 10^{-5} mol/L, *vtgAb* mRNA expression significantly increased with rising EE2 concentrations, peaking at 10^{-7} mol/L. However, the *vtgAb* mRNA levels decreased at a concentration of 10^{-6} and 10^{-5} mol/L EE2 compared to 10^{-7} mol/L. The relative *vtgAb* mRNA

expression induced by different EE2 concentrations began to increase significantly compared to the controls at 24 and 48 h, reached a peak at 72 h, and subsequently declined to lower levels by 96 h at all concentrations. The highest *vtgAb* mRNA expression in hepatocytes occurred at 72 h following exposure to 10^{-7} mol/L EE2, with expression levels approximately 30 times higher than the controls, which differs notably from the expression patterns observed in *S. argus* liver tissues (Figure 5).

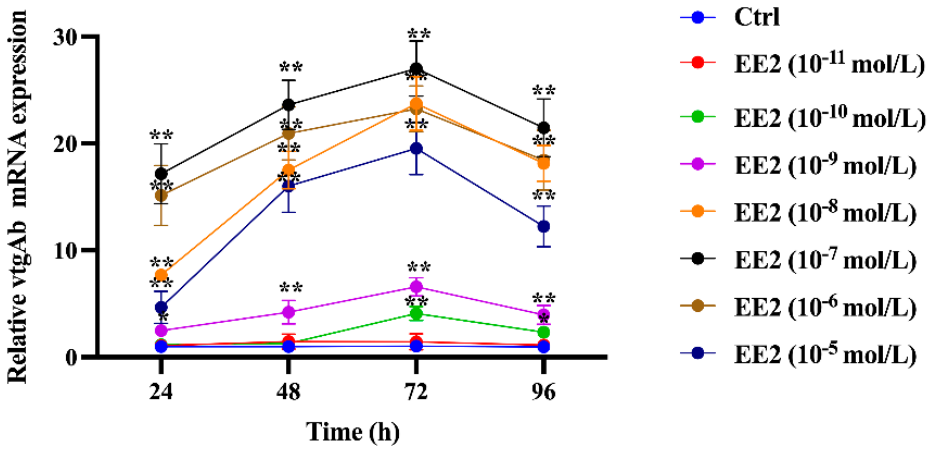

Figure 5. Analysis of *vtgAb* mRNA expression in *S. argus* hepatocytes after exposure to different concentrations of EE2 at different processing times in vitro. The asterisk above the data point represents significant difference, ** $p < 0.01$ vs. control (Ctrl).

4. Discussion

Vtg exhibits a range of additional functions beyond its role in yolk formation. Studies have demonstrated that purified Vtg can agglutinate the red blood cells of toads and chickens, suggesting that Vtg possesses agglutinin activity in teleost fishes [19,28]. Moreover, yolk protein, derived from Vtg, binds to lipids and lipid-soluble components, such as riboflavin, thyroxine, carotenoids, and vitamins, thereby facilitating their systemic transport and utilisation [7]. This lipid-binding functionality is further supported by findings in *Nematostella vectensis*, where Vtg interacts with Apolipoprotein B and Very-Low-Density Lipoprotein Receptors (VLDLRs) for the efficient distribution of fatty acids and other dietary nutrients, an evolutionarily conserved mechanism [29]. Additionally, yolk protein exhibits metal-chelating properties, binding to Cu^{2+}, Zn^{2+}, Fe^{2+}, and Fe^{3+} ions [30]. This capability not only facilitates essential mineral transport but may also play a role in antioxidant defence, as demonstrated in painted dragon lizards (*Ctenophorus pictus*), where Vtg counteracts oxidative stress during reproductive periods. Plasma Vtg levels in these lizards were positively correlated with reduced reactive oxygen species (ROS), particularly post-ovulation when oxidative stress peaks [31]. Furthermore, the hydrolysis of yolk protein in oocytes releases free AAs, which increases osmotic pressure and promotes oocytes hydration, a critical process during maturation [32]. This hydration mechanism is paralleled by the oocyte–endocytosis systems observed in crustaceans like shrimp (*Litopenaeus vannamei*), where Vtg receptor (VgR)-mediated Vtg uptake drives hydration and maturation, with RNA interference experiments showing a complete arrest of oocyte development upon VgR silencing [33].

Given these diverse functional roles, it is not surprising that *vtg* is encoded by a family of genes that exhibit considerable variation across species. In fish, the *vtg* gene family consists of multiple subtypes, with many such subtypes identified in different species [24]. The specific roles of these *vtg* subtypes may differ between species; however, no role-differentiated *vtg* subtypes have been identified in *S. argus* until now. In this study,

we used 5′ and 3′ RACE amplification to clone the full-length cDNA sequences of three *vtg* subtypes (*vtgAa*, *vtgAb*, and *vtgC)* from the liver of *S. argus*, confirming the existence of multiple Vtg proteins in this species. Our results also revealed divergent evolutionary rates among different functional regions of the *vtg* gene, with regions rich in serine having evolved rapidly, while highly conserved regions evolved much more slowly. This evolutionary variation shows the importance of exploring *vtg* subtypes in fish like *S. argus* to understand their evolutionary and functional adaptations.

In this study, we confirmed three Vtg subtypes in *S. argus*, VtgAa, VtgAb, and VtgC encoding 1696, 1699, and 1275 AA, respectively. The AA encoded by the three Vtg subtypes in *S. argus* showed the highest identity with *M. americana* (83%, 85%, and 85%). Similarly, the identity values with *P. major*, another species belonging to the order Perciformes, were 81%, 82%, and 83%, respectively. The phylogenetic analysis of Vtg in *S. argus* and six other species revealed that all three subtypes of Vtg in *S. argus* clustered closely with *M. americana* and *P. major*, supporting the conclusion that Vtg AA sequences are highly conserved in evolutionary relationships. Previous studies indicated that Vtg is hydrolysed into LvH, PV, and LvL in vertebrate oocytes [34]. In this study, we made a preliminary prediction of the structures of VtgAa, VtgAb, and VtgC in *S. argus* by comparing them with the structure domains of Vtg in *D. rerio*. The protein structures of VtgAa and VtgAb were found to be consistent with VtgAo2 in *D. rerio* [35], containing the complete structure of LvH, PV, and LvL. Also, VtgC possessed the full structure of LvH and LvL but lacked the PV domain, similar to *D. rerio* [34].

Vtg synthesis can occur through either endogenous or exogenous pathways [36]. Endogenous synthesis refers to the production of Vtg within the oocyte itself, while exogenous synthesis refers to the production of Vtg outside the oocyte, primarily in the liver. In fish, exogenous synthesis in the liver is the main pathway for Vtg production [37]. The synthesised Vtg is subsequently transported to the ovaries via the bloodstream, where it is stored in the oocytes to provide the necessary energy for embryonic development [37]. It has also been shown that ovarian follicular cells in *D. rerio* can synthesise Vtg [38], suggesting the potential for an endogenous Vtg synthesis pathway in fish. However, studies on *D. rerio* and *O. latipes* have indicated that *vtg* gene expression is restricted to the liver in female fish [39]. Research on the Sichuan bream (*Sinibrama taeniatus*) further demonstrated that the liver is the primary organ of *vtg* expression, with significantly higher expression levels compared to other organs [40]. In this study, we successfully cloned three *vtg* gene subtypes (*vtgAa*, *vtgAb*, and *vtgC*) from the liver of *S. argus* by *vtg* cDNA.

Previous studies have shown that the levels of *vtg* in the hepatocytes of teleost vary depending on their developmental stage [27,32]. For instance, in rainbow trout (*Oncorhynchus mykiss*), the *vtg* content was found to be lowest during the immature stage [27]. These findings suggest that immature teleosts may not synthesise substantial amounts of *vtg* endogenously, and the observed *vtg* production during these stages is likely induced by external factors, such as exposure to oestrogens, like EE2. qRT-PCR analysis in the current study revealed that *vtgAb* consistently showed a higher expression than the other *vtg* subtypes, with minimal expression at low EE2 doses (0.01 and 0.1 μg/g) but significant increases at higher doses (1.0 and 10.0 μg/g). In *D. rerio*, the greatest *vtg* mRNA expression occurred 48 h after the intraperitoneal injection of 5.0 μg/g EE2, with a 35-fold increase [41]. However, in our in vivo study, the highest expression of *vtgAb* in *S. argus* hepatocytes was observed 72 h after exposure to 10.0 μg/g EE2, with a relative increase of only about 3-fold. This suggests that *S. argus* exhibits a relatively strong tolerance to EE2. Based on these results, *vtgAb* was selected for the further in vitro analysis of mRNA expression levels.

In vitro, the effect of EE2 on *vtgAb* mRNA expression in primary cultured hepatocytes of *S. argus* was found to be both dose- and time-dependent. The expression was nearly undetectable at 10^{-11} mol/L but significantly increased between 10^{-10} and 10^{-5} mol/L, peaking at 10^{-7} mol/L after 72 h with approximately 30-fold. These in vitro results differed substantially from the in vivo experiments, where *S. argus* demonstrated a notable capacity to regulate exogenous hormones. It is hypothesised that this discrepancy arises because, in vivo, EE2 reaches the liver through blood circulation. During this circulation phase, EE2 is diluted by blood and bodily fluids before binding to the liver hormone receptor to stimulate Vtg synthesis. By the time EE2 interacts with the liver, its concentration would be lower than it was at the point of injection. In contrast, during the in vitro experiment, hepatocytes were directly exposed to EE2, allowing for immediate interaction with hormone receptors, leading to a higher level of *vtgAb* expression compared to the in vivo conditions.

5. Conclusions

In conclusion, and as further highlighted in Table 3, this study confirms that *S. argus* expresses three *vtg* subtypes (*vtgAa*, *vtgAb*, and *vtgC*), with *vtgAb* being the most responsive to oestrogen exposure. This research highlights the evolutionary conservation of Vtg proteins across species and shows the importance of exploring Vtg subtypes to understand their functional roles.

Table 3. Key findings of *vtg*/Vtg responses in *S. argus* to EE2 exposure with implications for environmental monitoring and future research.

Key Findings	Policy Implications	Research Recommendations
vtgAb shows the highest expression, with a 3-fold increase in vivo (10.0 μg/g EE2) and a 30-fold increase in vitro (10^{-7} mol/L EE2).	Prioritise *vtgAb* for monitoring oestrogenic pollutants due to its high sensitivity to EE2 exposure.	Expand *vtgAb* testing across fish species to validate its universality as a biomarker.
In vivo *vtgAb* expression peaks at 72 h post-injection with doses ≥ 1.0 μg/g EE2, showing significant dose-dependence.	Refine pollution monitoring to include time-sensitive sampling strategies targeting peak biomarker expression.	Investigate optimal sampling timelines for accurate assessment of EEDCs.
In vitro hepatocyte assays show peak *vtgAb* expression at 72 h with EE2 concentrations of 10^{-7} mol/L, declining at higher doses (10^{-6} and 10^{-5} mol/L).	Include dose–response assessments in regulatory standards to identify thresholds of pollutant impact.	Examine mechanisms of reduced biomarker expression at higher pollutant concentrations.
S. argus shows strong tolerance to EE2, with lower *vtgAb* upregulation in vivo compared to other teleost species (e.g., 3-fold vs. 35-fold in *D. rerio*).	Use *S. argus* as a reference species for resilience studies in regulatory assessments.	Explore genetic and physiological traits contributing to *S. argus* resilience to pollutants.
Identity analysis revealed that *S. argus* Vtg AA sequence share 85% identity with *M. americana* and 82% with *P. major*.	Apply findings to related teleost species for broader environmental monitoring strategies.	Conduct comparative studies to confirm biomarker applicability across species with high VtgAb identity.

Supplementary Materials: The following supporting information can be downloaded at: www.mdpi.com/xxx/s1, Figure S1. Sequences of *S. argus* Vtgs. Signal peptide: rectangular frame; the PV of VtgAa and VtgAb: shaded areas; LvL of VtgC: underlined areas.

Author Contributions: M.W. drafted the initial manuscript. D.W. and J.Z. conducted the analysis of specific experimental data. A.S.M. contributed to the development and refinement of the manuscript. W.W. designed the experimental protocol and supervised the entire experimental

process and assisted in revising the initial draft. All authors have read and agreed to the published version of this manuscript.

Funding: The current research was financially supported by the National Key Research and Development Program of China, 2022YFE0203900; National Natural Science Foundation of China (41506193).

Institutional Review Board Statement: The animal study protocol adhered to the ethical guidelines of Shanghai Ocean University (approval number SHOU-DW-2024-093) for the care and use of experimental animals throughout the experimental procedures.

Data Availability Statement: Data available on request from the authors.

Acknowledgments: The authors wish to acknowledge Junbin Zhang, Shenzhen University, for his advice on the experimental design.

Conflicts of Interest: The authors declare that there are no conflicts of interest.

References

1. Du, B.H.; Fan, G.D.; Yu, W.W.; Yang, S.; Zhou, J.J.; Luo, J. Occurrence and risk assessment of steroid oestrogens in environmental water samples: A five-year worldwide perspective. *Environ. Pollut.* **2020**, *267*, 115405.
2. Stiefel, C.; Stintzing, F. Endocrine-active and endocrine-disrupting compunds in food-occurrence, formation and relevance. *Nfs J.* **2023**, *31*, 57–92.
3. Zhao, X.M.; Grimes, K.L.; Colosi, L.M.; Lung, W.S. Attenuation, transport, and management of oestrogens: A review. *Chemosphere* **2019**, *230*, 462–478.
4. Xiong, W.L.; Peng, W.L.; Fu, Y.L.; Deng, Z.X.; Lin, S.J.; Liang, R.B. Identification of a 17β-estradio-degrading *Microbacterium hominis* SJTG1 with high adaptability and characterization of the genes for oestrogen degradation. *J. Hazard. Mater.* **2023**, *444*, 130371.
5. Rose, E.; Paczolt, K.A.; Jones, A.G. The effects of synthetic oestrogen exposure on premating and postmating episodes of selection in sex-role-reversed Gulf pipefish. *Evol. Appl.* **2013**, *6*, 1160–1170.
6. Sun, S.X.; Wu, J.L.; Lv, H.B.; Zhang, H.Y.; Zhang, J.; Limbu, S.M.; Qiao, F.; Chen, L.Q.; Yang, Y.; Zhang, M.L.; et al. Environmental oestrogen exposure converts lipid metabolism in male fish to a female pattern mediated by AMPK and mTOR signaling pathways. *J. Hazard. Mater.* **2020**, *394*, 122537.
7. Matozzo, V.; Gagné, F.; Marin, M.G.; Ricciardi, F.; Blaise, C. Vitellogenin as a biomarker of exposure to oestrogenic compounds in aquatic invertebreates: A review. *Environ. Int.* **2008**, *34*, 531–545.
8. Muller, M.; Rabenoelina, F.; Balaguer, P.; Patrueau, D.; Lemenach, K.; Budzinski, H.; Barceló, D.; Alda, M.L.; Kuster, M.; Delgenès, J.P.; et al. Chemical and biogical analysis of endocrine-disrupting hormones and oestrogenic activity in an advanced sewage treatment plant. *Environ. Toxicol. Chem.* **2008**, *27*, 1649–1658.
9. Wang, W.W.; Lian, Q.P.; Chen, Y.G.; Hiramatsu, N.; Wu, M.Q. Development and characterization of polyclonal antibodies against subtype specific vitellogenin of the dojo loach, *Misgurnus anguillicaudatus*. *Aquaculture* **2021**, *532*, 736089.
10. Rutherford, R.; Lister, A.; Bosker, T.; Blewett, T.; Meina, E.G.; Chehade, I.; Kanagasabesan, T.; MacLatchy, D. Mummichog (*Fundulus heteroclitus*) are less sensitive to 17α-ethinylestradiol (EE_2) than other common model teleosts: A comparative review of reproductive effects. *Gen. Comp. Endocr.* **2020**, *289*, 113378.
11. Toan, N.K.; Ahn, S.G. Aging-related metabolic dysfunction in the salivary gland: A review of the literature. *Int. J. Mol. Sci.* **2021**, *22*, 5835.
12. Rosati, L.; Chianese, T.; Simoniello, P.; Motta, C.M.; Scudiero, R. The Italian wall lizard *Podarcis siculus* as a biological model for research in male reproductive toxicology. *Int. J. Mol. Sci.* **2022**, *23*, 15220.
13. Shi, Y.; Yao, G.; Zhang, H.; Jia, H.X.; Xiong, P.P.; He, M.X. Proteome and transcriptome analysis of gonads reveals intersex in *Gigantidas haimaensis*. *BMC Genom.* **2022**, *23*, 174.
14. Hiramatsu, N.; Hara, A.; Hiramatsu, K.; Fukada, H.; Weber, G.M.; Denslow, N.D.; Sullivan, C.V. Vitellogenin-derived yolk proteins of shite perch, Morone americana: Purification, characterization, and vitellogenin-receptor binding. *Biol. Reprod.* **2002**, *67*, 655–667.

15. Sawaguchi, S.; Kagawa, H.; Ohkubo, N.; Hiramatus, N.; Sullivan, C.V.; Matsubara, T. Molecular characterization of three forms of vitellogenin and their yolk protein products during oocyte growth and maturation in red seabream (*Pagrus major*), a marine teleost spawning pelagic eggs. *Mol. Reprod. Dev.* **2006**, *73*, 719–736.
16. Hiramatsu, N.; Matsubara, A.; Fujita, T.; Sullivan, C.V.; Hara, A. Multiple piscine vitellogenins: Biomarkers of fish exposure to oestrogenic endocrine disruptors in aquatic environments. *Mar. Biol.* **2006**, *149*, 35–47.
17. Amano, H.; Fujita, T.; Hiramatsu, N.; Sawaguchi, S.; Matsubara, T.; Sullivan, C.V.; Hara, A. Purification of multiple vitellogenins in grey mullet (*Mugi cephalus*). *Mar. Biol.* **2007**, *152*, 1215–1225.
18. Ohkubo, N.; Andoh, T.; Mochida, K.; Adachi, S.; Hara, A.; Matsubara, T. Deduced primary structure of two forms of vitellogenin in Japanese common goby (*Acanthogobius flavimanus*). *Gen. Comp. Endocr.* **2004**, *137*, 19–28.
19. Fujiwara, Y.; Fukada, H.; Shimizu, M.; Hara, A. Purification of two lipovitellins and development of immunoassays for two forms of their precursors (vitellogenins) in medaka (*Oryzias latipes*). *Gen. Comp. Endocr.* **2005**, *143*, 267–277.
20. Sawaguchi, S.; Koya, Y.; Yoshizaki, N. Multiple vitellogenins (Vgs) in mosquitofish (*Gambusia affinis*): Identification and characterization of three functional Vg genes and their circulating and yolk protein products. *Biol. Reprod.* **2005**, *72*, 1045–1060.
21. MacLatchy, D.L.; Courtenay, S.C.; Rice, C.D.; Kraak, G.J.V. Development of a shrot-term reproductive endocrine bioasay using steroid hormone and vitellogenin end points in the estuarine mummichog (*Fundulus heteroclitus*). *Environ. Toxicol. Chem.* **2003**, *22*, 996–1008.
22. Ndiaye, P.; Forgue, J.; Lamothe, V.; Cauty, C.; Tacon, P.; Lafon, P.; Davail, B.; Fostier, A.; LE Menn, F.; Núñez, J. Tilapia (*Oreochromis mossambicus*) vitellogenins: Development of homologous and heterologous ELISAs and analysis of vitellogenin pathway through the ovarian follicle. *J. Exp. Zool. A Comp. Exp. Biol.* **2006**, *305*, 576–593.
23. Zhong, Y.; Duan, Z.Y.; Su, M.L.; Lin, Y.Q.; Zhang, J.B. Inflammatory responses associated with hyposaline stress in gill epithelial cells of the spotted scat *Scatophagus argus*. *Fish. Shellfish. Immu.* **2021**, *114*, 142–151.
24. Petersen, T.N.; Brunak, S.; Heijne, G.V.; Nielsen, H. SIGNALP 4.0: Discriminating signal peptides from transmembrane regions. *Nat. Methods* **2011**, *8*, 785–786.
25. Figueiredo, N.; Matos, B.; Diniz, M.; Branco, V.; Marins, M. Marine fish primary hepatocyte isolation and culture: New insights to enzymatic dissociation pancreatin digestion. *Int. J. Environ. Res. Public Health* **2021**, *18*, 1380.
26. Gui, L.; Zhang, P.P.; Zhang, Q.Y.; Zhang, J.B. Two hepcidins from spotted scat (*Scatophagus argus*) possess antibacterial and antiviral functions *in vitro*. *Fish. Shellfish. Immu.* **2016**, *50*, 191–199.
27. Hultman, M.T.; Rundberget, J.T.; Tollefsen, K.E. Evaluation of the sensitivity, responsiveness and reproducibility of primary rainbow trout hepatocyte vitellogenin expression as a screening assay for oestrogen mimics. *Aquat. Toxicol.* **2015**, *159*, 233–244.
28. Shi, X.; Zhang, S.; Pang, Q. Vitellogenin is a novel player in defense reactions. *Fish. Shellfish. Immu.* **2006**, *20*, 769–772.
29. Lebouvier, M.; Miramón-Puértolas, P.; Steinmetz, P. Evolutionary conserved aspects of animal nutrient uptake and transport in sea anemone vitellogenesis. *Curr. Biol.* **2022**, *32*, 4620–4630.
30. Samaraweera, H.; Zhang, W.G.; Lee, E.J.; Ahn, D.U. Egg yolk phosvitin and functional phosphopeptides-review. *J. Food. Sci.* **2011**, *76*, R143–R150.
31. Lindsay, W.; Friesen, C.; Sihlbom, C.; Bergström, J.; Berger, E.; Wilson, M.; Olsson, M. Vitellogenin offsets oxidative costs of reproduction in female painted dragon lizards. *J. Exp. Biol*. **2020**, *223*, 221630.
32. Finn, R.N.; Fyhm, H.J. Requirement for amino acids in ontogeny of fish. *Aquac. Res.* **2010**, *41*, 684–716.
33. Ruan, Y.; Wong, N.; Zhang, X.; Zhu, C.; Wu, X.; Ren, C.; Luo, P.; Jiang, X.; Ji, J.; Wu, X.; et al. Vitellogenin Receptor (VgR) Mediates Oocyte Maturation and Ovarian Development in the Pacific White Shrimp (*Litopenaeus vannamei*). *Front. Physiol*. **2020**, *11*, 485.
34. Finn, R.N.; Kristoffersen, B.A. Vertebrate vitellogenin gene duplication in relation to the "3R hypothesis": Correlation to the pelagic egg and the oceanic radiation of teleosts. *PLoS ONE* **2007**, *2*, e169.
35. Zhong, L.Q.; Yuan, L.; Rao, Y.; Li, Z.Q.; Zhang, X.H.; Liao, T.; Xu, Y.; Dai, H.P. Distribution of vitellogenin in zebrafish (*Danio rerio*) tissues for biomarker analysis. *Aquat. Toxicol.* **2014**, *149*, 1–7.
36. Kong, H.J.; Kim, J.L.; Moon, J.Y.; Kim, W.J.; Kim, H.S.; Park, J.Y.; Cho, H.K.; An, C.M. Characterization, expression profile, and promoter analysis of the *Rhodeus uyekii* vitellogenin *Ao1* gene. *Int. J. Mol. Sci.* **2014**, *15*, 18804–18818.
37. Nath, P.; Sahu, R.; Kabita, S. Vitellogenesis with special emphasis on Indian fishes. *Fish. Physiol. Biochem.* **2007**, *33*, 359–366.
38. Liu, K.C.; Wu, R.; Ge, W. Luteinizing hormone receptor (*lhcgr*) as a marker gene for characterising oestrogenic endocrine-disrupting chemicals in zebrafish ovarian follicle cells. *Gen. Comp. Endocr.* **2013**, *192*, 89–94.
39. Tong, Y.; Shan, T.; Poh, Y.; Yan, T.; Wang, H.; Lam, S.H.; Gong, Z.Y. Molecular cloning of zebrafish and medaka vitellogenin genes and comparison of their expression in response to 17 β-estradiol. *Gene* **2004**, *328*, 25–36.

40. Zhao, Z.; Zhao, Q.; Wang, H.Y.; Wei, L.; Wang, S.Y.; Li, S.L.; Yuan, D.Y.; Wang, Z.J. Integrated transcriptomic and metabolomic analyses identify key factors in the vitellogenesis of juvenile Sichuan bream (*Sinibrama taeniatus*). *Front. Mar. Sci.* **2023**, 1243767.
41. Bowman, C.J.; Kroll, K.J.; Hemmer, M.J.; Folmar, L.C.; Denslow, N.D. Oestrogen-induced vitellogenin mRNA and protein in sheepshead minnow (*Cyprinodon variegatus*). *Gen. Comp. Endocr.* **2000**, *120*, 300–313.